

CALIBRATING ANISOTROPIC VELOCITY MODELS FOR VACA MUERTA

DANIEL O. PÉREZ^{1,2,3}, SOLEDAD R. LAGOS^{1,2}, DANILO R. VELIS^{1,2} and JUAN C. SOLDÓ³

¹ *Facultad de Ciencias Astronómicas y Geofísicas - Universidad Nacional de La Plata, La Plata, Argentina. dperez@fcaglp.unlp.edu.ar; velis@fcaglp.unlp.edu.ar*

² *CONICET, La Plata, Argentina. slagos@fcaglp.unlp.edu.ar*

³ *Ecopetrol, Bogota, Colombia. juan.c.soldo@ecopetrol.com.co*

(Received August 22, 2018; revised version accepted August 12, 2019)

ABSTRACT

Pérez, D.O., Lagos, S.R., Velis, D.R. and Soldo, J.C., 2019. Calibrating anisotropic velocity models for Vaca Muerta. *Journal of Seismic Exploration*, 28: 495-511.

We provide well-calibrated VTI velocity models useful to locate microseismic events in the Vaca Muerta shale formation, Neuquén, Argentina. Assuming layered models with weak anisotropy, we make use of the information provided by well logs and perforation shots of known position to estimate the layer velocities, depths and anisotropy. This leads to a constrained nonlinear inverse problem that consists of minimizing the discrepancies between the observed and calculated P- and S-wave arrival time differences. To avoid local minima and other convergence issues, we minimize the resulting objective function using very fast simulated annealing (VFSA). We test the proposed strategy on field data and estimate a set of velocity models that honor the observed data, which we validate carrying out a simulated microseismic event location. The results show that the proposed strategy is capable of estimating layered VTI velocity models suitable to accurately locate microseismic events during a hydraulic stimulation in the Vaca Muerta shale formation.

KEY WORDS: VTI, Vaca Muerta, microseismic, calibration, velocity model, VFSA.

INTRODUCTION

Unconventional reservoirs, such as the Vaca Muerta shale formation in Argentina, are mainly composed of intrinsically extremely low permeability rocks, in which hydrocarbon exploitation is difficult and expensive (Rauzi et al., 2014). In order to enhance production this type of reservoirs requires hydraulic stimulation to create pathways connecting the isolated hydrocarbon with the well bore, increasing permeability. The pressure increment induced by the hydraulic stimulation can produce slippage along weakness planes in the reservoir rocks near the treatment well (Warpinski et al., 2005). The activation of pre-existing fractures and the creation of new ones produce microseismic activity and the consequent propagation of compressional and shear seismic waves which are recorded at the surface, shallow boreholes or nearby wells. The arrival times of these waves can be measured and the location of the aforementioned slippages can be inferred, given a velocity model (Maxwell, 2014).

The fracture mapping is of paramount importance in the exploitation of the reservoir and in the planning of new exploration wells (Downton and Gray, 2006; Chen et al., 2012; Liu and Martinez, 2012; Mahmoudian et al., 2013; Bachrach, 2014; Maxwell, 2014). In order to correctly characterize the hydraulically stimulated region, the location of the microseismic events should be as accurate as possible. However, uncertainties associated with the location exist, and have several causes. One cause is the inability to accurately detect the compressional and shear-waves arrivals at a sufficient number of receivers, because the number of receivers is often very limited and the coverage is poor. Moreover, the accuracy of the first arrival picking decreases as the noise level increases. Another cause is the difficulty to adequately determine the velocities at which the seismic waves propagate through the medium (Warpinski et al., 2005). The seismic velocities within a reservoir are affected by numerous parameters such as the porosity, fluid content, pressure, and temperature. In addition, the underlying medium often shows an anisotropic behavior, a property that most sedimentary rocks exhibit at a significant degree. Anisotropy can be consequence of many complex factors such as natural fractures, thin layering, the alignment of the crystalline structure of the minerals within the rocks, or regional structural stress.

Velocity models apparently suitable for event location can be derived from well log data. However, most common logging tools only measure vertical velocities and their use can lead to large errors in the location of the microseismic events, because these values are not reliable away from the well (Maxwell et al., 2010). Furthermore, logging tools do not provide enough information to properly characterize anisotropy. To obtain good location results it is necessary to calibrate the velocity models using the information provided by some type of calibration shot, such as a perforation shot, a string shot or a drop ball. Unlike the microseismic events, the

location of the calibration shot is well known, and the estimation of the velocity model can be carried out by solving an inverse problem whose solution is non-unique (Akram and Eaton, 2013). The correct characterization of the subsurface anisotropy can lead to accurate event location estimates, as we will show in the examples section.

In this work we propose an inversion strategy to calibrate anisotropic velocity models. We assume that the subsurface is composed of a finite number of vertical transverse isotropic (VTI) horizontal layers. Moreover, we consider "weak" anisotropy, a widely used approximation that leads to the so-called Thomsen parameters (Thomsen, 1986). Given a known seismic source, the discrepancies between the observed and calculated arrival times difference between the compressional and share waves are quantified by means of an objective function that depends on the vertical velocities, the Thomsen parameters and the interfaces depths. The layering of the media and the effect of the various parameters on the traveltime calculations result in a discontinuous, non-linear, and multimodal cost function. To avoid local minima and convergence issues, we minimize it using very fast simulated annealing (VFSA) (Ingber, 1989), a stochastic global optimization algorithm devised to find near-optimal solutions to hard optimization problems.

As is well-known, most geophysical inverse problems are inherently non-unique and ill-posed, for there exists several solutions that honor the data equally well. In particular, the use of microseismic data challenges even more the inversion process due its low signal-to-noise ratio and deficient acquisition geometries. For the sake of stabilization and to avoid meaningless solutions, appropriate constraints must be imposed. To this end, we use anisotropy constraints following the works of Mizuno et al. (2010) and Leaney et. al. (2014a). This allows us to set a relationship between the Thomsen parameters and the velocities, considerably reducing the ambiguity of the problem.

Several authors have developed methods to calibrate isotropic and anisotropic velocity models with very interesting and useful results. Warpinski et al. (2005) and Pei et al. (2009) horizontally layered isotropic velocity models from perforation shots. The former authors use multiple linear regression to build a system of equations from where the various parameters are obtained, while the latter authors use VFSA as in this work. Bardainne and Gaucher (2010) solve the eikonal equation and use simulated annealing to constrain isotropic velocity models with dipping interfaces and velocity gradients. Pei et al. (2014) and Li et al. (2014) propose to use the Levenberg-Marquardt algorithm to solve a linearized inversion scheme. The former to only estimate VTI models and the latter to also estimate, given enough *a priori* information, the locations of the microseismic events. In all cases, and in contrast to the method proposed in this work, the thickness of the layers are fixed.

This paper is organized as follows. First, we introduce the necessary theoretical background and make a detailed description of the inversion strategy. Next we test the method on microseismic field data from the Vaca Muerta shale formation. In the numerical example we estimate a group of anisotropic velocity models using a perforation shot of known location. The results show that the proposed strategy is capable of estimating velocity models with constrained values of the anisotropy parameters that honor the observed data. Then, we validate the solutions carrying out a simulated microseismic event location using, as microseismic events, several perforation shots that were not used during the inversion. The results show that the estimated models are appropriate to locate microseismic events, providing locations close to the actual ones. Finally, the Conclusions section summarizes the main results.

THEORY

Anisotropy can be consequence of several complex factors, such as the preferred orientation of minerals grains, the bedding of isotropic fine layers or the presence of vertical or dipping fractures and micro-cracks. This leads to various anisotropic types that depend on the resulting symmetry systems at seismic wavelengths. Transverse isotropy (TI) is perhaps the most important type of anisotropy (Sheriff and Geldart, 1995), being VTI due to nearly horizontal layering a typical example of shale formations (Thomsen, 1996) such as Vaca Muerta (Willis, 2003). Other anisotropy types arise when a vertical or tilted fracture system is superposed to a VTI medium, leading to orthorhombic or monoclinic anisotropy (Tsvankin, 2012). In general, the anisotropy due to the horizontal layering is much stronger than the anisotropy due to the fracture system (Sheriff and Geldart, 1995). Then, in this work we rely on the hypothesis that the subsurface is composed of a finite number of homogeneous horizontal layers of known thickness, showing VTI.

The calibration strategy that we propose starts with the construction of a layered isotropic velocity model from a sonic log in a nearby well, usually the monitoring well. To this end, we use the multivariate zonation algorithm proposed by Velis (2007, 2010). Given a fixed number of interfaces, this algorithm automatically obtains a layered model for the seismic velocities. In practice, the zonation into relatively homogeneous and stationary velocity intervals is driven by the statistical behavior of the data.

Only five independent parameters are necessary to characterize VTI media (Backus, 1962; Berryman, 1979; Thomsen, 1986; Yilmaz, 2001). The most basic representation of these parameters are the five independent elastic constants of the stiffness tensor derived from Hooke's law (Aki and

Richards, 1980; Lay and Wallace, 1995). This representation leads to seismic velocities equations that make the development of inversion algorithms difficult, and challenge the qualitative estimation of the anisotropy effects. To overcome these drawbacks, Thomsen (1986) redefined the anisotropy parameters obtaining the following expressions for the seismic velocities:

$$v_P(\theta) = v_{P0}(1 + \delta \sin^2 \theta \cos^2 \theta + \epsilon \sin^4 \theta) \quad , \quad (1)$$

$$v_{SH}(\theta) = v_{S0}(1 + \gamma \sin^2 \theta) \quad , \quad (2)$$

$$v_{SV}(\theta) = v_{S0} \left(1 + \frac{v_{P0}^2}{v_{S0}^2} (\epsilon - \delta) \sin^2 \theta \cos^2 \theta \right) \quad , \quad (3)$$

where v_P is the compressional or P-wave velocity, v_{SV} and v_{SH} are the slow-shear or SV- and fast-shear or SH-wave velocities, respectively, and θ is the angle between the propagation direction and the symmetry axis, which in VTI media is vertical. In addition ϵ , δ and γ are the so-called Thomsen parameters, which are dimensionless, while v_{P0} and v_{S0} denote the corresponding P- and S-wave vertical velocities.

Given a seismic source and an array of n_r geophones, both with known positions, we want to determine the properties of the medium from the recorded arrival times of P-, SV- and SH-waves. This inversion problem is carried out by minimizing the following cost function:

$$J(\mathbf{m}) = \left\{ \frac{1}{n_r} [\|(\mathbf{t}_P + \mathbf{T}_0) - \mathbf{T}_P\|_2^2 + \|(\mathbf{t}_{SH} + \mathbf{T}_0) - \mathbf{T}_{SH}\|_2^2 + \|(\mathbf{t}_{SV} + \mathbf{T}_0) - \mathbf{T}_{SV}\|_2^2] \right\}^{\frac{1}{2}} \quad , \quad (4)$$

where \mathbf{m} is the model vector than contains the information of the vertical velocities v_P and v_S , the interfaces depths \mathbf{z} and the Thomsen parameters ϵ , δ and γ of the layers. The vectors \mathbf{t} and \mathbf{T} of dimension n_r are the calculated traveltimes and observed arrival times of P, SH and SV phases. T_0 is the origin time of the perforation shot, and is equal for all phases. Naturally, in order to minimize inaccuracies in the estimated model and in the localization of microseismic events, errors in \mathbf{T}_0 must be kept to a minimum (Warpinski et al., 2005).

It is worth noting that sometimes T_0 is not known with enough accuracy or not known at all. In those cases, when it is not possible to use the eq. (4), we could use the following cost function:

$$J(\mathbf{m}) = \left\{ \frac{1}{n_r} [\|(\Delta \mathbf{t} - \Delta \mathbf{T})_{P-SH}\|_2^2 + \|(\Delta \mathbf{t} - \Delta \mathbf{T})_{P-SV}\|_2^2] \right\}^{1/2} \quad , \quad (5)$$

where vectors $\Delta \mathbf{t}$ and $\Delta \mathbf{T}$ of dimension n_r are the calculated traveltime differences and observed arrival times differences, respectively, for the indicated seismic phase pairs.

Since in any case $J(m)$ is discontinuous, multimodal and highly non-linear with respect to the unknowns m , we minimize it using very fast simulated annealing (VFSA) (Ingber, 1989), a stochastic global optimization algorithm that does not require the use of gradients or derivatives, avoids local minima and converges faster than other simulated annealing (SA) algorithms. The traveltimes calculation from the source to the receivers is *per se* a non-linear inverse problem that requires the use of iterative methods. In this work we calculate the traveltimes using an anisotropic ray-tracing algorithm (Pérez et al., 2016) adapted from the work of Tian and Chen (2005). As for the observed arrivals times, we use automated phase pickers (Sabbione and Velis, 2013; Velis et al., 2015).

Most geophysical inverse problems are non-unique and ill-posed because data is incomplete and inaccurate. As a result, there is not enough information from which reliably estimate a large number of unknowns. Furthermore, the trade-off between the Thomsen parameters and the seismic velocities in eqs. (1) to (3) increases the difficulties. All these issues can be alleviated by decreasing the number of unknowns and by adding geological constraints. For this purpose, we follow the method proposed by Mizuno et al. (2010) and assume that the anisotropy is driven by an auxiliary log. This allows us to write

$$\epsilon = \hat{\epsilon} \mathbf{c} \quad , \quad (6)$$

$$\delta = \hat{\delta} \mathbf{c} \quad , \quad (7)$$

$$\gamma = \hat{\gamma} \mathbf{c} \quad , \quad (8)$$

where $\hat{\epsilon}$, $\hat{\delta}$ and $\hat{\gamma}$ are scale factors. Each element of the vector \mathbf{c} is given by

$$\frac{c_i - c_{min}}{c_{max} - c_{min}} \quad , \quad i = 1, \dots, n_l \quad (9)$$

where c_i is the value of the auxiliary log in the i^{th} -layer, c_{min} and c_{max} are the minimum and maximum values, and n_l is the number of layers. In sand-shale systems using v_{p0}/v_{s0} as the auxiliary log is a good choice, since v_{p0}/v_{s0} is a good proxy for the volume of clay. In systems with carbonates, $1/v_p$ is a better choice to drive anisotropy (Mizuno et al., 2010; Leaney, 2014b).

The described strategy, of common use in the industry, helps to significantly mitigate the ambiguity problem by reducing the number of unknowns through geological constraints (Leaney, 2014b). In the new formulation, the unknown variables, assuming 1D subsurface, are the vertical velocities and v_{s0} , the interfaces depths z , and the three scale factors $\hat{\epsilon}$, $\hat{\delta}$ and $\hat{\nu}$. In practice, we initialize the vertical velocities and the interfaces depths using well-log information. To account for variations in the region between the perforation shots and the receivers, these parameters are also adjusted as part of the calibration process.

NUMERICAL EXAMPLE

We test the proposed calibration strategy using microseismic data registered during a hydraulic fracturing process carried out in the Vaca Muerta shale formation, Argentina. The Vaca Muerta formation (Weaver, 2013) contains the largest potential unconventional resources in Argentina. This unit covers more than 80000 km² of the Neuquén Basin which is a huge, oil and gas prolific basin including most of the Neuquén Province, western part of Río Negro and La Pampa Provinces and southwest portion of Mendoza Province. It was deposited during upper Jurassic to early Cretaceous (Middle Tithonian - Lower Berrasian), in a semi restricted basin connected with the Pacific Ocean. The Vaca Muerta sequences were originated in a mixed clastic and carbonatic system. Along the basin, Vaca Muerta's thickness varies from approximately from 20 to 600 m, strongly controlled by the space accommodation during depositional period. These variations make the unit extremely heterogeneous. In the study area, the thickness of the shale section consists of more than 350 m of marls with a variable content of carbonate/quartz and a low percentage of clays (5-19%). The TOC average in the upper section of the unit is 3.5% and in the lower section is among 6%. Porosity ranges from 6 to 11% in the whole section. Due the characteristics of Vaca Muerta formation we decide to use $1/v_{p0}$ as the auxiliary log in eq. (9).

Fig. 1 depicts the geometry of the monitoring and treatment wells, and the relative position of the considered sources and receivers. The sources comprise a set of five perforation shots, each one associated to a different hydraulic stimulation stage. The treatment well is almost horizontal at the perforation shots level, while the receivers were located in an approximately vertical monitoring well. The seven receivers were separated 30 m from each other, in a position slightly shallower than the shots. The distance along the treatment well trajectory between shots #1 and #5 was about 280 m, while the difference in depth was 75 m. The shot #1 was about 500 m away from the monitoring well, being the most distant one.

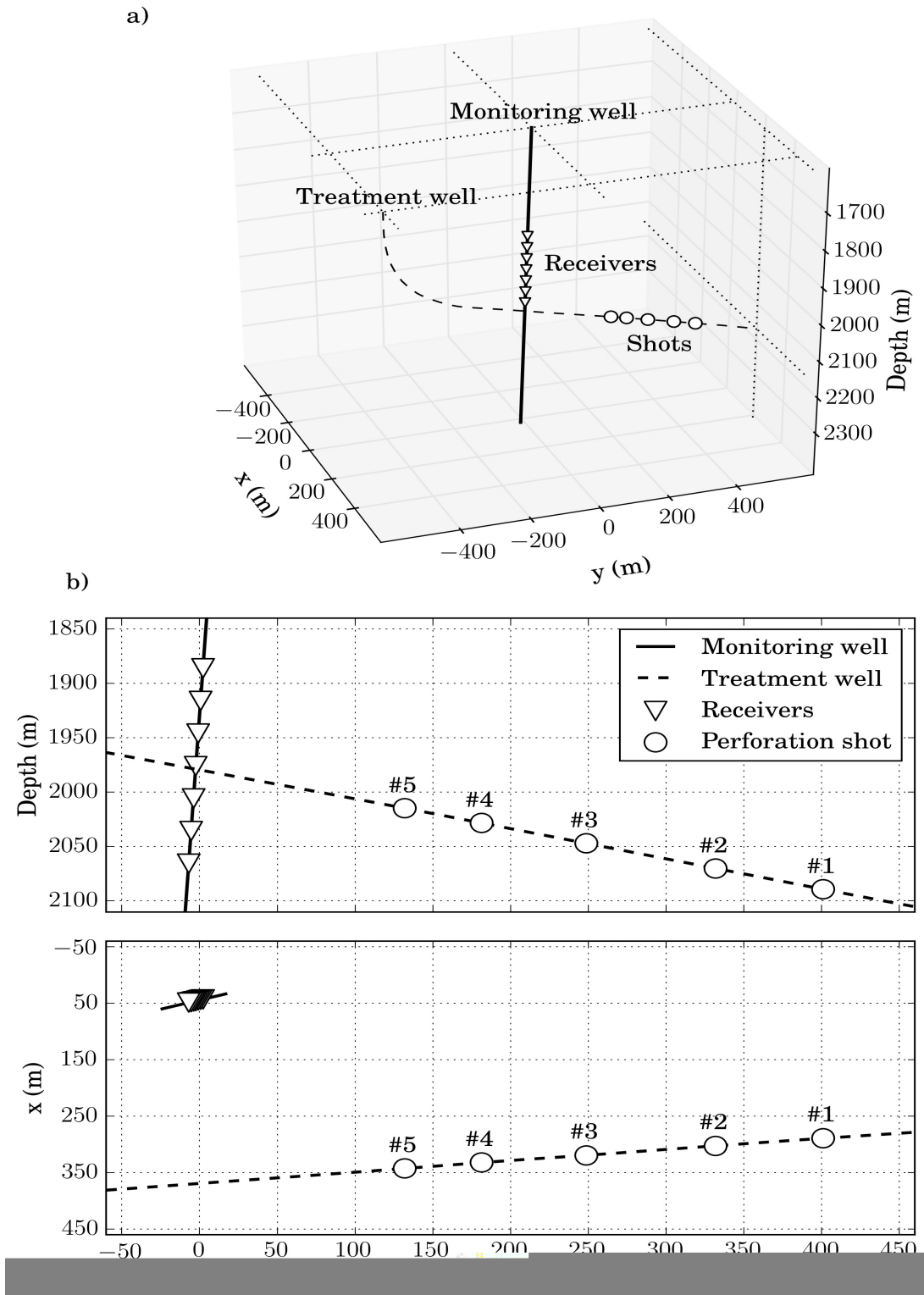


Fig. 1. (a) Configuration of the monitoring and treatment wells, and relative position of sources and receivers. (b) Projection of the wells onto the vertical and horizontal plane.

Fig. 2 shows the seismic data recorded during the five perforations shots and the corresponding arrival time picks. The similarity among the records suggests that the underlying geological structure exhibits small lateral variations. In all cases the quality of the data was high enough so as to easily detect and pick the P- and SH-waves arrivals, but not the corresponding SV-waves. For this reason, the terms of the cost function that depend on SV-waves arrival times were not used in the process. Also, since T_0 was not available we decide to perform the calibration using eq. (5).

To illustrate the proposed method, we carry out the following experiment. First, using the time picks from the perforation shot #1, we estimated a set of 100 anisotropic velocity models that honor the observed data within a given tolerance. Each model was obtained by minimizing eq. (4) via VFSA using a different seed for the pseudo-random number generator. Then, we located the remaining four perforation shots using their corresponding time picks. In a real world scenario, the model is usually re-calibrated after each new hydraulic stimulation stage. Subsequently, the microseismic events associated to that stage are located using the corresponding calibrated model. In this example we assumed that the perforations shots that were not used in the calibration were microseismic events to be located. Since the actual location of these events were known, this simulated location scenario allowed us to validate the estimated models.

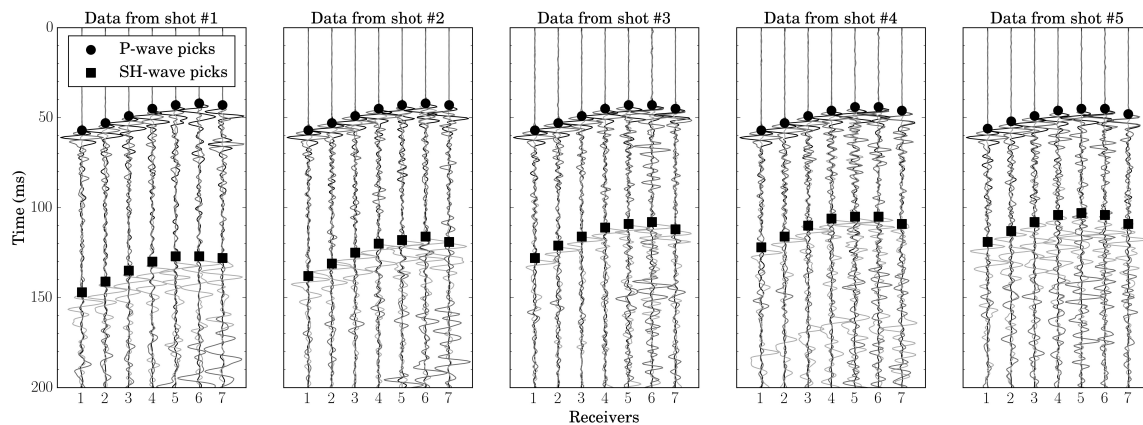


Fig. 2. Observed data and phase arrival picks corresponding to perforation shots #1 to #5.

In addition to the microseismic data, sonic log data acquired at the monitoring well was also available. We used this information to obtain the initial vertical velocities and interface depths. Fig. 3 shows a portion of a dipole sonic log acquired at the monitoring well. The gray curves are the P- and S-waves velocities measurements, while the continuous black curves are the layered model estimated by the multivariate zonation algorithm

proposed by Velis (2010). The dashed lines indicate the resulting interfaces. We used this model as an initial solution of the vertical velocities v_{P0} and v_{S0} and the interfaces positions \mathbf{z} .

During the calibration we allowed v_{P0} and v_{S0} to vary independently for each layer $\pm 1\%$ around the initial values given by the zonation algorithm. On the other hand, we allowed to vary the positions of the interfaces ± 10 m around their initial values. As for the scale factors $\hat{\epsilon}$ and $\hat{\gamma}$ we allowed them to vary in the range 0 to 0.3. Due to the relative positions of the perforation shots and the receivers, the seismic rays were nearly horizontal. In this scenario, seismic velocities are little sensitive to Thomsen parameter δ (Berryman et al., 1999; Djikpesse, 2014). Hence, the terms that contain δ in equations 1 to 3 were neglected. Following Eisner et al. (2010) we assumed Gaussian errors with $\sigma = 0.5$ ms for both the P- and SH-time picks. Thus, the VFSA iterative process stopped when the cost function reached this value.

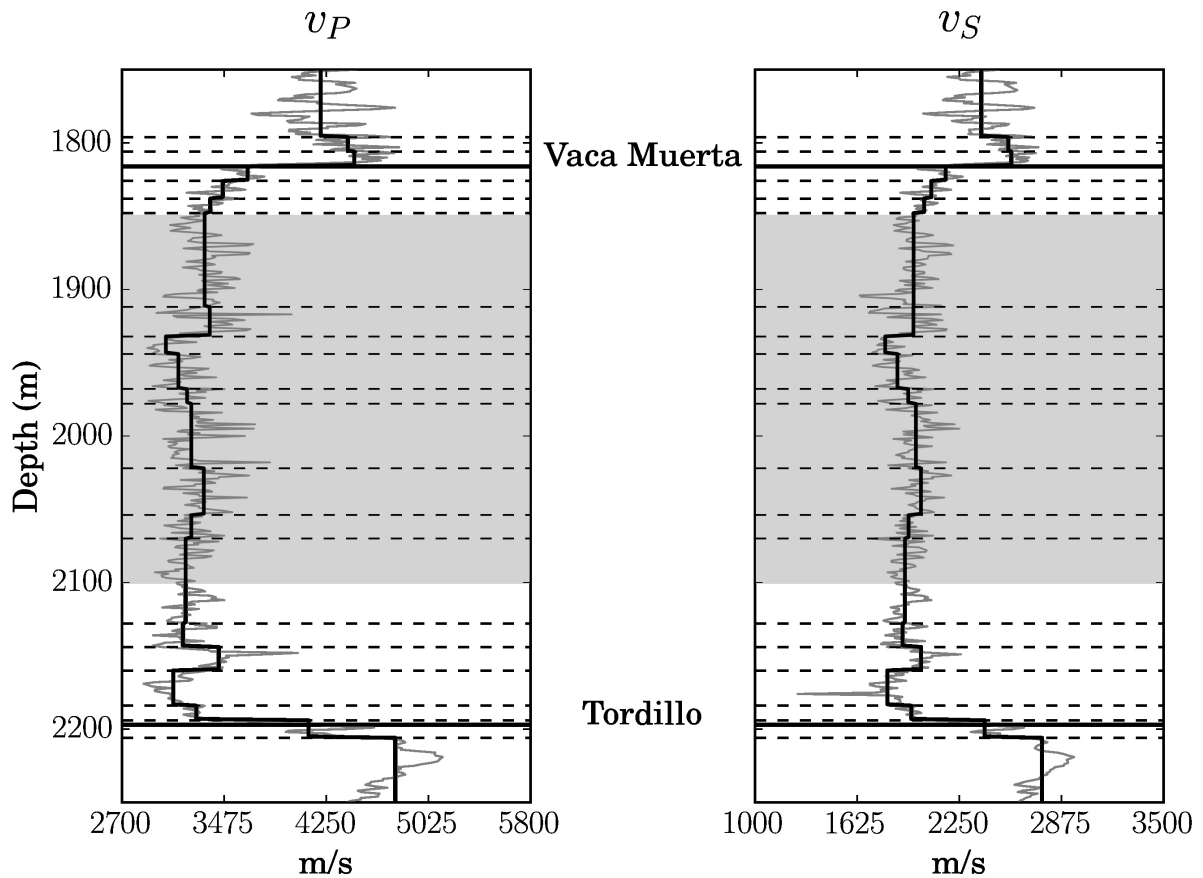


Fig. 3. Gray lines: V_P and V_S measured from a sonic log in the monitoring well. Black lines: V_P and V_S estimated using the zonation algorithm. Gray area: range where the model is calibrated.

Fig. 4 shows the results of 100 runs of the calibration process. As expected, the interface depths and the vertical velocities show little variation, according to the rather small search ranges. On the other hand, the relatively large dispersions of the estimated anisotropy parameters reveal that, despite the fact that all the calibrated models honor the observed data within the required precision (Fig. 4e), the non-uniqueness of the problem persists. From the 100 realizations of the VFSA we estimated a value of $\hat{\epsilon} = 0.118 \pm 0.043$, and a value of $\hat{\gamma} = 0.144 \pm 0.025$.

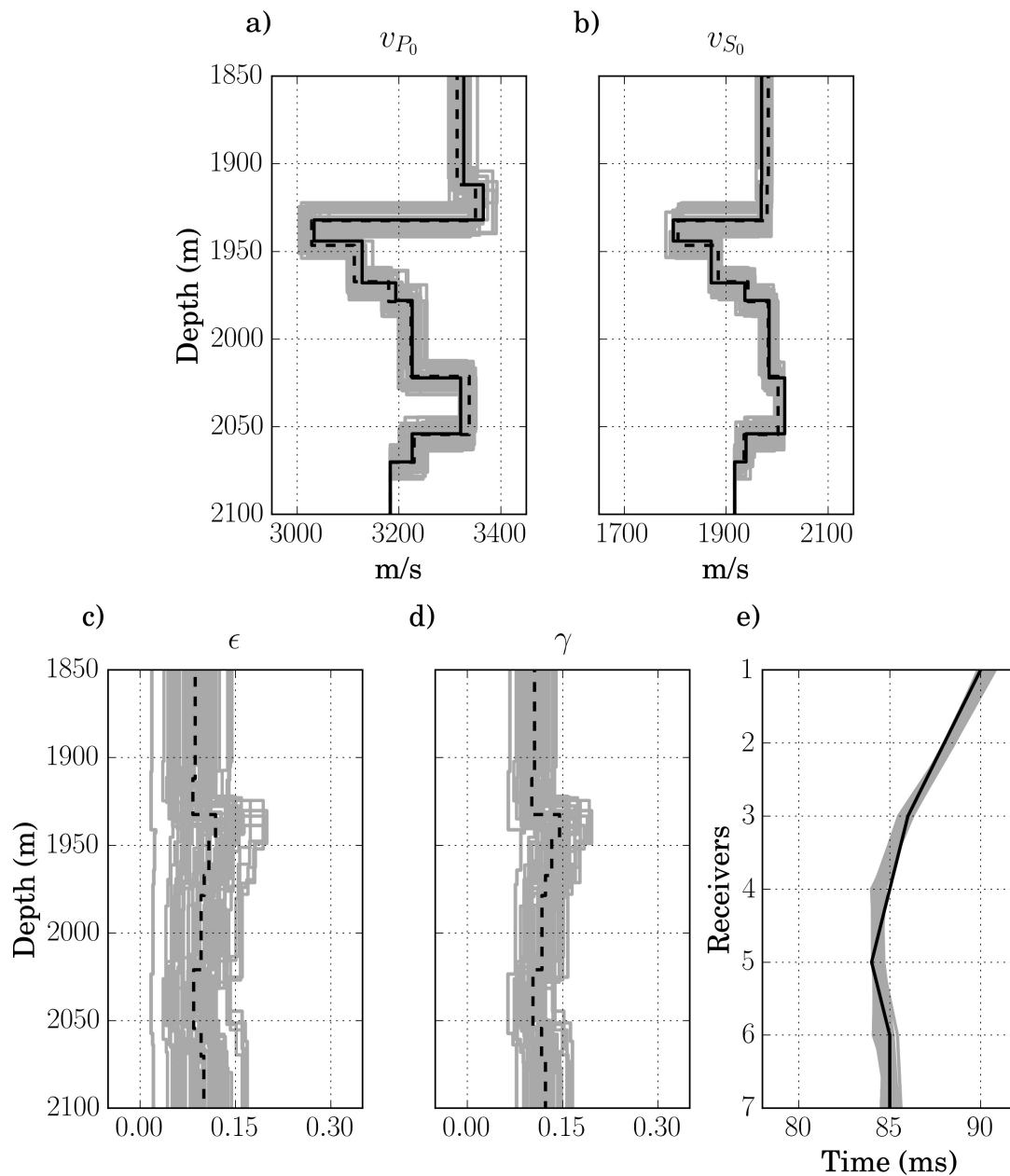


Fig. 4. (a) to (d) velocities and Thomsen parameters for the 100 estimated models (graylines) and their mean values (dashed black lines). (e) Estimated (gray) and observed (black) difference times curves.

Given the 100 calibrated models using the time picks of shot #1 (Fig. 2, first panel), the second part of the experiment consisted on the location of shots #2 to #5, whose positions are known, using their corresponding time picks (Fig. 2, panels two to five). Likewise the calibration problem, the localization problem relied on the minimization of the same cost function [eq. (4)] where the unknowns were the shot coordinates instead of the velocities and the anisotropy scale factors. For VTI media, the perforation shot coordinates can be defined by three parameters: backazimuth, distance from the receiver, and depth. For a single monitoring well, as in the case of this work, the cost function given by eq. (4) does not depend on the backazimuth. Thus, we estimated this parameter previously via a polarization analysis, which leads to an optimization problem with two unknowns, only. In practice, we set the SA search ranges of the distance from the receiver and depth to (0,1000) m and (1500,2200) m, respectively. We used the same stopping criteria of the iterative process as in the calibration. To assess the importance of well-calibrated velocity models, and for the sake of comparison, we also located the shots using the layered isotropic model shown in Fig. 3.

Fig. 5 shows the location results for the 100 calibrated models for shots #2 to #5. In general, the locations were successful. Despite their differences (see Fig. 4), all the models led to shot locations within tolerable errors. In all cases, the uncertainties in depth were larger than those in the horizontal direction, as expected. This behavior can be explained by the fact that the relative positions of shots and receivers promoted rather horizontal rays, thus increasing the depth uncertainties. For the shots closer to the receivers, as shots #4 and #5, the rays were more oblique and the depth uncertainties decreased. The locations using the isotropic layered model were far from acceptable.

Table 1. Actual coordinates of the shots and errors in the estimated coordinates using the isotropic and anisotropic model. For the anisotropic case we show the mean value and standard deviation of the errors from the 100 realization.

Shot	Actual		Isotropic		Anisotropic	
	Dist. (m)	Depth (m)	Δ Dist. (m)	Δ Depth (m)	Δ Dist. (m)	Δ Depth (m)
#2	419.6	2070.0	-45.0	-48.0	3.51 ± 1.85	4.42 ± 5.67
#3	370.0	2047.0	-51.7	-92.1	1.93 ± 1.45	-2.18 ± 8.24
#4	340.3	2028.3	-47.5	-78.9	7.97 ± 1.72	-7.72 ± 3.62
#5	326.5	2014.7	-43.1	-65.8	13.24 ± 1.70	-10.65 ± 2.67

Table 1 summarizes the values of the estimated errors relative to the actual coordinates of the shots (distance from the receivers and depth) for each located shot. The accuracy of the solutions obtained using the anisotropic models clearly are superior to those obtained using the isotropic model. For all perforation shots the estimated mean values were only a few meters away from the actual values, showing small standard deviations. These results highlight the importance of having well-calibrated subsurface models that include anisotropy. Finally, and for the sake of completeness, Fig. 6 shows the observed and calculated time differences for the 100 locations associated to each shot. The curves show that all models and perforation shot coordinates honor the observations accurately.

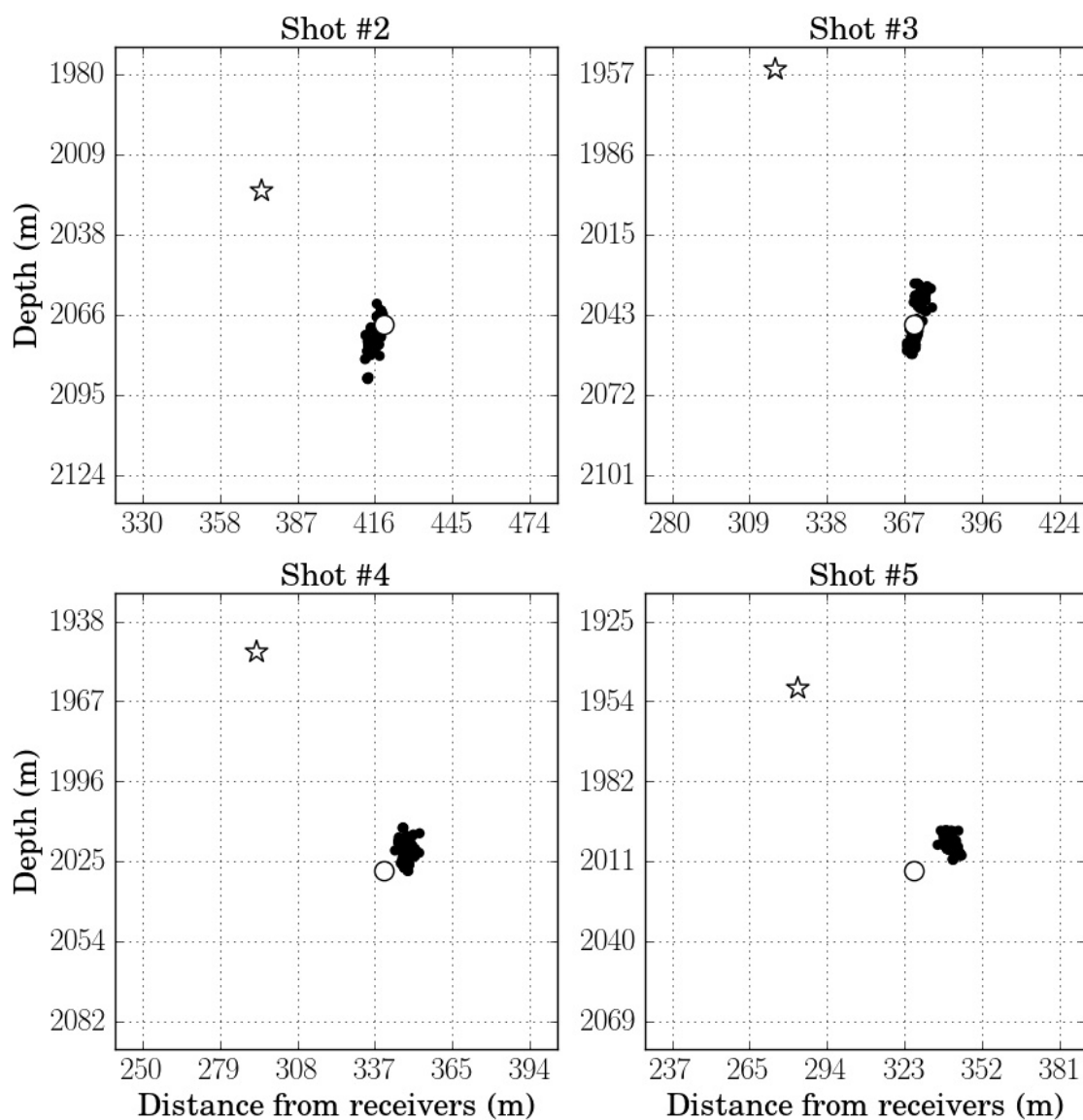


Fig. 5. Location of shots #2 to #5 using the 100 estimated models (black dots), actual shot position (white dots), and estimated location using the isotropic model (white stars).

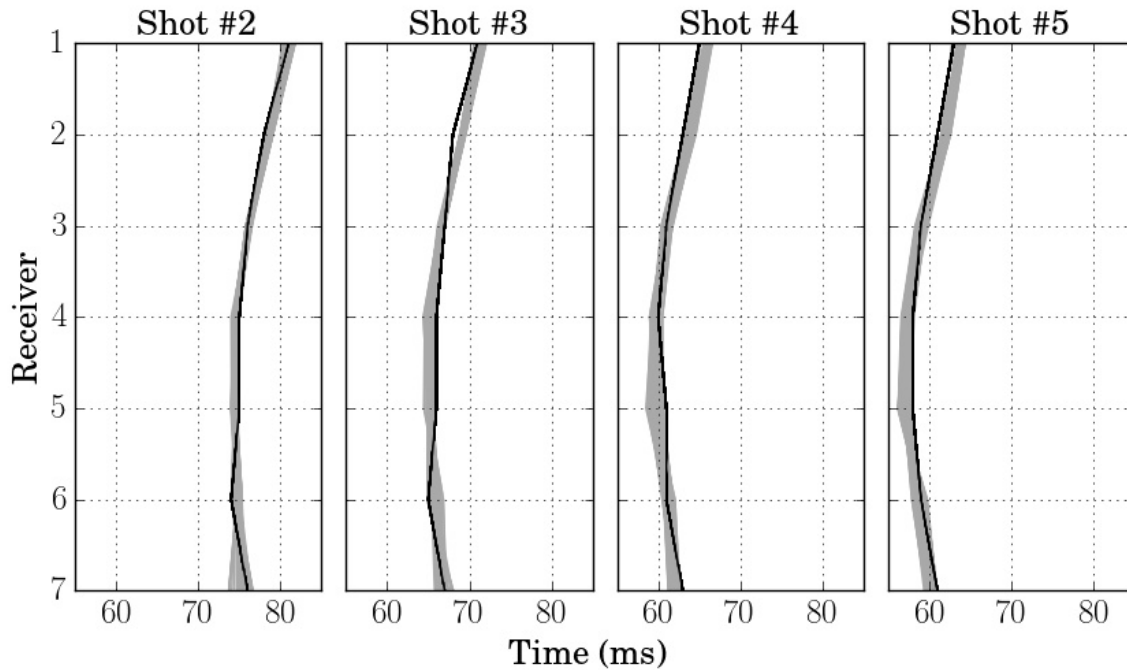


Fig. 6. Estimated (gray) and observed (black) time differences curves corresponding to the 100 locations of shots #2 to #5.

CONCLUSIONS

The proposed strategy allowed us to calibrate useful anisotropic velocity models from perforation shots records. This microseismic data was acquired at a single monitoring well in the Vaca Muerta shale formation, Neuquén, Argentina, during a hydraulic fracturing procedure. The strategy relied on the use of VFSA to minimize an appropriate non-linear cost function, which included the calibration of the vertical velocities, the anisotropy scale factors, and the interfaces depths. We estimated the uncertainties of the estimated solutions by virtue of the stochastic nature of VFSA. The use of geological constraints associated to the Thomsen parameters led to a significant reduction of the non-uniqueness problem.

We applied the proposed method to obtain 100 calibrated models using the data from a single shot. The results showed that the strategy is capable of estimating a set of solutions with an acceptable dispersion that honor the observed data very accurately. We assessed the solutions by location tests using data from the perforations shots not used in the calibrations. Despite the dispersion in the estimated models and the limited amount of available data and poor ray coverage, the locations were successful. As expected, the errors in the locations increased with the distance from the shots to the receivers, but in all cases these errors were

acceptable (smaller than 15 m). For comparison, we also located the perforation shots using the isotropic layered model derived from log data at the monitoring well. In this case, the estimated locations were far from acceptable, showing large errors in both vertical and horizontal coordinates. This result highlights the importance of having appropriate subsurface models that take into account the anisotropy to locate microseismic events in Vaca Muerta.

ACKNOWLEDGMENTS

We are grateful to the Consejo Nacional de Investigaciones Científicas y Técnicas (CONICET) and YPF Tecnología S.A. for their support. We are also grateful to Germán I. Brunini and Dr. Emilio Camilión for fruitful discussions and comments. Our thanks also to the reviewer and the editor for their constructive comments and valuable suggestions

REFERENCES

- Aki, K., and P. Richards, 1980, *Quantitative Seismology: Theory and Methods*. W.H. Freeman and Co., Sausalito.
- Akram, J. and Eaton, D., 2013. Impact of velocity model calibration on microseismic locations. Expanded Abstr., 83rd Ann. Internat. SEG Mtg., Houston: 1982-1986.
- Bachrach, R., 2014. Linearized orthorhombic AVAz inversion: Theoretical and practical consideration. Expanded Abstr., 84th Ann. Internat. SEG Mtg., Denver: 528-532.
- Backus, G.E., 1962. Long-wave elastic anisotropy produced by horizontal layering. *J. Geophys. Res.*, 67: 4427-4440.
- Bardainne, T. and Gaucher, E., 2010. Constrained tomography of realistic velocity models in microseismic monitoring using calibration shots. *Geophys. Prosp.*, 58: 739-753.
- Berryman, J.G., 1979, Long-wave elastic anisotropy in transversely isotropic media. *Geophysics*, 44: 896-917.
- Berryman, J.G., Grechka, V.Y. and Berge, P.A., 1999. Analysis of Thomsen parameters for finely layered VTI media. *Geophys. Prosp.*, 47: 959-978.
- Chen, H., Zhang, G. and Yin, X., 2012. AVAz inversion for elastic parameter and fracture fluid factor. Expanded Abstr., 82nd Ann. Internat. SEG Mtg., Las Vegas: 1-5.
- Cooke, D. and Schneider, W., 1983. Generalized linear inversion of reflection seismic data. *Geophysics*, 48: 665-676.
- Corona, W.W. and Mavko, G., 2008. In: *Predicting Clay Content and Porosity from Gamma-ray and Conductivity Logs*: 425-433.
- Djikpesse, H.A., 2015. C_{13} and Thomsen anisotropic parameter distributions for hydraulic fracture monitoring. *Interpretation*, 3: SW1-SW10.
- Downton, J. and Gray, D., 2006. AVAz parameter uncertainty estimation. Expanded Abstr., 76th Ann. Internat. SEG Mtg., New Orleans: 234-238.
- Eisner, L., Hulsey, B.J., Duncan, P., Jurick, D., Werner, H. and Keller, W., 2010. Comparison of surface and borehole locations of induced seismicity. *Geophys. Prosp.*, 58: 809-820.

- Ingber, L., 1989. Very fast simulated re-annealing. *J. Mathemat. Computat. Modell.*, 12: 967-973.
- Lay, T. and Wallace, T.C., 1995. *Modern Global Seismology*. Academic Press, New York.
- Leaney, S., Chapman, C. and Yu, X., 2014a. Anisotropic moment tensor inversion, decomposition and visualization. *Expanded Abstr.*, 84th Ann. Internat. SEG Mtg., Denver: 2250-2255.
- Leaney, S., 2014b. *Microseismic Source Inversion in Anisotropic Media*. Ph.D. thesis, University of British Columbia, Vancouver, BC.
- Li, J., Li, C., Morton, S.A., Dohmen, T., Katahara, K. and Toksöz, M.N., 2014. Microseismic joint location and anisotropic velocity inversion for hydraulic fracturing in a tight bakken reservoir. *Geophysics*, 79: C111-C122.
- Liu, E. and Martinez, A., 2012. *Seismic Fracture Characterization, Concepts and Practical Applications*. EAGE, Houten.
- Mahmoudian, F., Margrave, G.F., Wong, J. and Henley, D.C., 2013. Fracture orientation and intensity from AVAz inversion: A physical modeling study. *Expanded Abstr.*, 83rd Ann. Internat. SEG Mtg., Houston: 483-487.
- Maxwell, S., Bennett, L., Jones, M. and Walsh, J., 2010. In: *Anisotropic Velocity Modeling for Microseismic Processing: Part 1 - Impact of Velocity Model Uncertainty*. SEG, Tulsa, OK: 2130-2134.
- Mizuno, T., Leaney, S. and Michaud, G., 2010. Anisotropic velocity model inversion for imaging the microseismic cloud. *Extended Abstr.*, 72nd EAGE Conf., Barcelona.
- Pei, D., Carmichael, J., Waltman, C. and Warpinski, N., 2014. Microseismic anisotropic velocity calibration by using both direct and reflected arrivals. *Expanded Abstr.*, 84th Ann. Internat. SEG Mtg., Denver: 2278-2282.
- Pei, D., Quirein, J.A., Cornish, B.E., Quinn, D. and Warpinski, N.R., 2009. Velocity calibration for microseismic monitoring: A very fast simulated annealing (vfsa) approach for joint-objective optimization. *Geophysics*, 74, WCB47-WCB55.
- Pérez, D.O., Lagos, S.R., Velis, D.R. and Soldo, J.C., 2016. Inversion of seismic anisotropic parameters using very fast simulated annealing with application to microseismic event location. *Mecánica Computacional*, Vol. XXXIV, Asociación Argentina de Mecánica Computacional: 3351-3367.
- Rauzi, R.S., Santiago, M.F., Alvarado, O.A. and Bertoldi, F., 2014. Estrategia de terminación y ensayo del primer pozo exploratorio no convencional de la formación Vaca Muerta en la subcuenca de Picún Leufí. Neuquén, Argentina. Presented at the IX Congreso de Exploración y Desarrollo de Hidrocarburos.
- Rider, M. and Kennedy, M., 2011. *The Geological Interpretation of Well Logs*. Rider-French, Cambridge.
- Sabbione, J.I. and Velis, D.R., 2013. A robust method for microseismic event detection based on automatic phase pickers. *J. Appl. Geophys.*, 99: 42-50.
- Sheriff, R.E. and Geldart, L.P., 1995. *Exploration Seismology*, 2nd Ed., Cambridge University Press.
- Thomsen, L., 1986. Weak elastic anisotropy. *Geophysics*, 51: 1954-1966.
- Tsvankin, I. 2012. *Seismic Signatures and Analysis of Reflection Data in Anisotropic Media*, 3rd Ed. SEG, Tulsa, OK..
- Velis, D.R., Sabbione, J.I. and Sacchi, M.D., 2015. Fast and automatic microseismic phase-arrival detection and denoising by pattern recognition and reduced-rank filtering. *Geophysics*, 80: WC25-WC38.
- Velis, D.R., 2003. Estimating the distribution of primary reflection coefficients. *Geophysics*, 68: 1417-1422.
- Velis, D.R., 2007. Statistical segmentation of geophysical log data. *Mathemat. Geol.*, 39: 409-417.
- Velis, D.R., 2010. Multivariate zonation of logging data. In: *Advances in Environmental Research*, 2. Nova Science Publishers Inc., Hauppauge, NY: 349-365.

- Walden, A. and Hosken, J., 1986. The nature of the non-Gaussianity of primary reflection coefficients and its significance for deconvolution. *Geophys. Prosp.*, 34: 1038-1066.
- Warpinski, N.R., Sullivan, R.B., Uhl, J., Waltman, C. and Machovoie, S., 2005. Improved microseismic fracture mapping using perforation timing measurements for velocity calibration. *SPE J.*, 10: 14-23.
- Weaver, C.E., 1931. *Paleontology of the Jurassic and Cretaceous of west and central Argentina*. University of Washington Press., Seattle, WA.
- Willis, M., 2013. Upscaling anisotropic geomechanical properties using Backus averaging and petrophysical clusters in the Vaca Muerta. M.Sc. Thesis, Colorado School of Mines, Golden, CO.
- Yilmaz, O., 2001, *Seismic Data Analysis: Processing, Inversion, and Interpretation of Seismic Data*. SEG Investigations in Geophysics. Tulsa, OK.
- Yue, T. and Chen, X.-F., 2005. A rapid and accurate two-point ray tracing method in horizontally layered velocity model: *Acta Seismol. Sin.*, 18: 154-161.